# Lateral Force Acting on the Sliding Spool of Control Valve Due to Radial Flow Force and Static Pressure

**QIANQIAN LU** [1], **JONNA TIAINEN** [2], **MEHRAN KIANI-OSHTORJANI** [2], **AND YANGFANG WU** [1]

[1]School of Engineering, Zhejiang University City College, Hangzhou, Zhejiang 310015, China
[2]School of Energy Systems, LUT University, 53850 Lappeenranta, Finland

Corresponding author: Yangfang Wu (wuyf@zucc.edu.cn)

**ABSTRACT** The hydraulic sliding-spool valve is a key component to control the flow rates and thus pressures in different hydraulic volumes. The lateral force on the spool is one of the important effects resulting from moving resistance. This paper presents research aimed at understanding the effects of radial flow force and static pressure upon the lateral force. The radial flow force is calculated from three types of control surfaces labelled with square land, 45° conical, and round curved surfaces, for discovering the effects of control profile, combined with inlet and outlet control conditions. The pressure difference effect is analyzed along with six cases under the same orifice opening, and the radial flow force is found to vary linearly with the pressure difference. The results also indicate that the radial force for the inlet control mode is less than that of the outlet control mode. The jet angle is discovered to not only be related to the annular orifice opening and gap clearance, but is also influenced by the flow direction and control surface profile. The static pressure is the predominant factor in the lateral force compared to the radial flow force. The results indicate that the static pressure variation on the surface of the cylindrical spool shoulder increased linearly with the inlet pressure; and two stagnation points can be observed in the case of the valve cavity with oil passages on the same section, and square land control edge profile. The lateral force on the spool increases with the pressure, and could reach to the maximum of 300 N, implying that this force should be taken into account in the selection of an actuator, especially in high pressure applications.

**INDEX TERMS** Flow force, jet angle, lateral force, sliding-spool valve, static pressure.

## I. INTRODUCTION

Flow force is often considered as one of the critical factors affecting the performance of a hydraulic control unit. A hydraulic spool valve with a spool sliding along its axial, is used to control flow direction, or flux by manipulating spool position or displacement. When the annular orifice formed by the spool land and housing is opened by a small size, the liquid flows through the orifice causing the flow velocity to change. Therefore, there is a flow force acting on the spool because of the time variation in fluid momentum.

The flow forces are usually divided into steady-state and transient flow forces. However, the transient flow force as often been ignored because it was smaller than the steady flow force and the pressure force [1], [2]. Many researchers have

The associate editor coordinating the review of this manuscript and approving it for publication was Agustin Leobardo Herrera-May [ID].

focused on the axial steady-state flow force because it is one of the axial components that the actuator should overcome. The expressions of steady-state and transient flow forces can be used to obtain the equation of motion of the valve spool. This equation of motion has been used to calculate the axial flow forces acting on the spool of the directional control valves, and compensates for the flow forces [3]. The importance of reducing the flow forces has been illustrated [4] when the flow forces are acting on the valve piston of the hydraulic sliding-spool valve, under high flow rate and pressure conditions. The compensation method has been presented [4] for inlet control edge, by modifying the sliding spool with a conical form on the inlet control edge. While for the outlet control edge, it has been demonstrated by designing a conical surface on the inner side of the valve socket at the outlet port, to conduct the outlet oil jet back to the slide spool. The spool profile of a hydraulic directional valve for compensation was

also studied [5], and a corrected equation to calculate flow force while considering the static pressure distribution in the valve cavity and pressure loss in nozzles was created [6]. The flow forces between the traditional square land spool, and the turbine-bucket spool, were compared by conducting experiments [6]. The results indicated that the flow force was influenced by the attachment of the jet to the spool, and the beveled spool compensated for the flow force, because of the high and unbalanced pressure acting on the upstream from the valve's orifice [7]. Other compensation methods were created by increasing the structure damping. The spool structure for instance, was optimized by adding a damping tail to compensate for the flow force acting on the spool, without affecting the pressure drop between the inlet and the outlet passages [8]. In similar work [9], a damping flange on the spool of the same cartridge valve was designed to decrease the axial flow force by 93 percent in the experimental test. In addition, flow force could be reduced by modifying the non-metering port geometry which improved the agility of the single stage electrohydraulic valves [10].

Besides the optimization of the spool structure by use of the compensation method, the axial flow force of a one-directional valve was also simulated [11], [12], and it was found that the flow velocity values were influenced by the spool displacement. The flow force was also found to be more influenced by the valve opening, than by the temperature of the flow servo valve used for the fuel metering unit [13].

The above-mentioned studies focused on the axial component of the steady-flow force, because it acts in the opposite direction to the drive force, and should be overcome during the work process. Thus, researchers have been trying to minimize the axial force in order to improve the power-to-weight ratio of the hydraulic control unit.

However, there exist frictional and inertial forces which are effective against the drive forces [2], [4] except for the flow force in a hydraulic spool valve. The reduction of the inertial force can only be achieved through a reduction in the mass of the moving components. The friction forces however, consist of the Coulomb friction produced by the viscosity friction and radial forces. The former exists when the spool is located in the exact centre of the bore, with constant radial clearance over the entire periphery. The latter appears when the spool is axially aligned but with eccentricity, tilt, as well as the profile machining error, such as the taper of the spool land. The taper spool contributes to the increase of the radial forces when the pressure at the larger end of the shoulder is higher than at the smaller end [3]. In addition, the contaminated friction of the clearance fit between the spool and its bore was also studied through the experiments [14]. The contaminated friction was increased on the cis-conical spool, but was decreased on the invert cone spool [14]. The contamination friction can be prevented by using a fine filter and by improving the machining accuracy.

The frictional forces can prevent the spool from moving, this phenomenon is called a hydraulic lock. The spool stroke mechanism of a pressure servo valve was investigated by considering the static-sliding friction, gap flow theory, and the flow force when the spool had the tendency to tilt axially [15]. The experimental test results of static friction forces acting on the spool of a hydraulic directional control valve loaded with axial and flow forces have been presented [16]. The results indicated that the frictional forces depend on the axial forces acting on the spool [16].

The forces derived from the liquid stream acting on the valve spool of directional control valve were computed [17], and the results indicated that the flow forces acting perpendicular to the spool axially were 40 N, and 28 N at the inlet passage in the directions along the port and normal to the port axes, respectively. The forces were 252 N, and 83 N for the outlet passage, when the flow rate was 450 l/min. These results demonstrated that flow forces acting perpendicular to spool axis should not be neglected, especially when calculating the driving force of the valve, as the force acting radially results in increasing friction. However, a detailed analysis was not provided [17].

So far, many researchers [4]–[7] have assumed that the radial flow force cancels itself out because of the assumption that the structure is symmetrical, and hence the radial flow force balance being zero. Actually, the three dimensional flow cavity inside the valve is not completely symmetrical, because the hydraulic valve should be arranged according to either the pipe systems, or valve block. Most of the hydraulic directional control valves are subplate-mounted so that the location of the oil ports are machined on the installation surface according to the ISO standards [18], resulting in unbalanced pressure, and velocity distributions around the cylindrical surfaces of the spool, as well as the annular orifices formed by the spool and sleeve (housing). The unbalanced radial component will force the spool against the bore, and the Coulomb friction forces may cause the spool to stroke.

Numerical simulation can provide important information about the jet angle values and the flow rate distribution inside the valve, in order to assist in obtaining precise flow force. The flow forces acting on the spool of an open-center hydraulic directional control valve were studied through experiments, CFD simulation, and theoretical analysis [19]. It was found that the maximum value of flow force appeared when the recirculating flow vanished, and the peak value of flow force occurred at the same opening around 2.4 mm, and the value increased along with the increasing pump flow rate [20]. The importance of using full 3D fluid dynamics analysis was emphasized [21], to more accurately evaluate the flow forces in a hydraulic directional proportional valve than it would in 2D and simplified 3D models. The structure of the sliding spool was modified to reduce the actuation forces [22].

The radial flow force at the annular orifice acting on the sliding spool with a conical side surface of a two-dimensional valve was studied numerically [23]. The results [23] demonstrated that the radial flow force increases with both the decreasing valve opening and increasing inlet flow velocity,

and the net flow force should be considered when calculating resistant forces. However, the study [23] did not consider the effects of control edge profiles, flow directions, or oil passage locations on the radial flow force.

This paper aims to fill the above-mentioned research gap, by experimentally, and numerically studying the effects of control edge profiles, flow direction, and oil passage locations on radial flow force. The hydraulic test bed was built to measure the pressure distribution of the 3D-printed tested valves with specific test channel, and the commercial software, ANSYS Fluent, is used as the numerical approach for calculating detailed information. For simulation, three different profiles of control edge are selected and are labeled as square land, 45 ° conical, and rounding curved surfaces as shown in Fig. 1. The first one is the traditional control edge of the sliding spool, the second type is designed to compensate for axial flow force [4], and the third one is the partial shape of the turbine profile used as control edge to reduce axial flow force [6]. As in the directional control valve, the flow should be free to flow in and out, so the influence of flow direction on the radial flow force is worth studying. In addition, the effect of the oil ports' location should be investigated as it has a direct effect on the asymmetry of the fluid cavity inside the valve.

This study sheds some light on the resistance forces of the sliding-spool valve. In addition, the results of this study indicate that the compensation of flow force in the axial direction only, is not enough to improve the power output of electro-mechanical actuator, without considering additional resistances.

The paper firstly introduces geometries of a sliding valve, and study cases in this research work. The fluid domain of each case is then built, and the CFD methodology introduced. After that, the results are shown based on different control edge profiles, flow directions, and distributions of oil passages. The discussion then proceeds with the results to illustrate the radial flow force distribution, and the effects of lateral force, as well as the effect caused by static pressure on the spool. The experimental setup for testing static pressure distributions was followed with the comparison of the experimental and simulation results. Lastly, the conclusions are provided.

## II. RADIAL STEADY FLOW FORCE AT ANNULAR ORIFICE

### A. GEOMETRIES

Flow force is known as the force induced by flow velocity. As for spool type valve, when the orifice opens, the fluid is able to flow into or discharge out of the cavity through the annular orifice as shown in Fig. 2. The flow direction changes at the orifice, and the pressure difference is generated according to the Bernoulli effect [24]. Moreover, the flow velocity increases as the flow stream narrows at the orifice, resulting in apparent flow force acting on the spool. The control edge of a sliding spool acting as a resistance, is defined as the inlet control edge when the fluid enters into the chamber, and the control edge is defined as the outlet control when the fluid
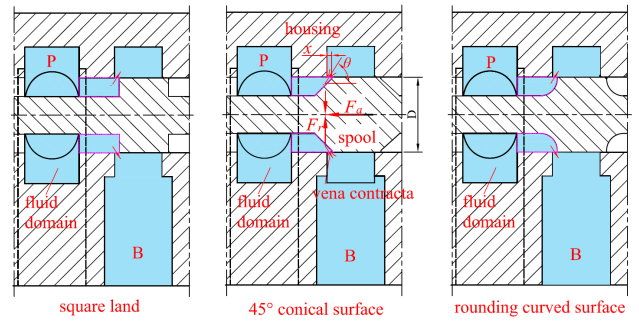


**FIGURE 1.** The sections of three control edge profiles of the spool installed inside standard housing labelled with square land, 45 ° conical surface, and rounding curved surface from left to right, respectively.
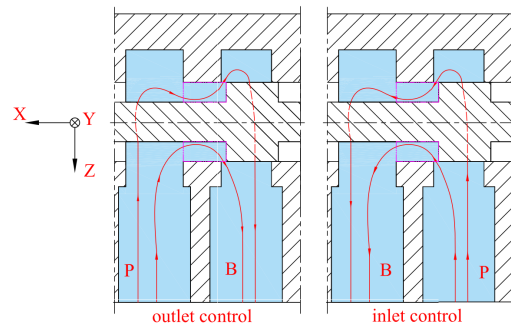


**FIGURE 2.** The sections of spool valves with oil passages located on the symmetric section. The left shows discharging out (outlet control), and the right is defined as entry in (inlet control).

discharges from the chamber. For commonly used four-way three-position directional valve, the four ports are machined onto the same installation surface according to ISO standards [18], resulting in the inlet, outlet, and work ports being situated in different sections, as seen in Fig. 1. The valve chamber structure whose inlet and outlet ports are located on the same cross section as the spool axis is studied in many occasions, when calculating axial flow force [4], [7] which is chosen for comparative analysis with the former valve.

The traditional geometry shape of the spool is machined with the square land shoulder, shown in Fig. 1 (left). The conical and partial turbine compensated profiles are shown in Fig. 1 (middle and right). This figure depicts the conical surface with an angle of 45°, and a round, curved surface, putting into consideration the machining costs. The parameters of the valves' geometries are listed in Table 1.

**TABLE 1.** The structure parameters of the valve.

| Name | Parameter | Value [ m ] |
|---|---|---|
| inlet port diameter | $d_{in}$ | 0.02 |
| outlet port diameter | $d_{out}$ | 0.02 |
| diameter of the rod | $d_{rod}$ | 0.011 |
| diameter of the shoulder | $d_s$ | 0.024 |
| depth of the groove | $e$ | 0.007 |
| width of the groove | $w$ | 0.011 |
| orifice opening | $x$ | $5 \times 10^{-4}$ |

### B. RADIAL FLOW FORCE AT ANNULAR ORIFICE

The expression of flow force was derived from the law of continuity, and the Bernoulli equation [25]. In the past, the axial flow force along the spool axis has been studied by neglecting
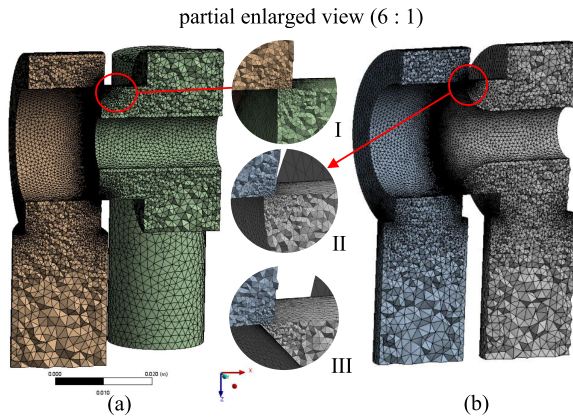
partial enlarged view (6 : 1)



I

II

III

(a)                                              (b)

**FIGURE 3.** Computational domain and grid.(a) the asymmetric control volume, (b) the symmetric control volume. Control surface: I - square land, II - rounding control, III - 45° conical control.

the radial component. However, the existence of radial flow force should be considered. It could be compensated for to some extent, even though not in full as proven by Rajda and Lisowski [17]. The radial flow force could be expressed as Eq.(1) with the direction perpendicular to the spool axis.

$$F_r = 2C_q C_v \pi d_s x \Delta p \sin\theta \tag{1}$$

where, $F_r$ is the radial flow force, in newtons (N); $C_q$ is the flow coefficient, $C_v$ is the velocity coefficient, $\Delta p$ is the pressure difference in pascals (Pa), which is calculated by subtracting outlet pressure from inlet pressure for the control volume, and $\theta$ is the jet angle referring to the acute angle between the velocity at the vena contracta, and the $X$ direction, shown in Fig. 2.

Here, the radial flow distribution along the annular orifice is considered by assuming that the spool axis is co-axial to the bore, which means that the effect of the radial force is directly related to the pressure difference, and the jet angle according to Eq.(1). Besides these two effects, the location of the oil ports contributes to the pressure distribution at the orifice, which should be considered [23]. The flow direction referred to as entry in, or discharge out from the cavity also has an influence over the flow force according to [4].

## III. NUMERICAL MODELING

### A. COMPUTATIONAL DOMAIN AND MODELING
The parameters, shown in Table 1, were used to build the finite-element model of the valve fluid domain. The 3D fluid asymmetric control volume was chosen to analyze the radial flow force at the annular orifice of the sliding valve. The computational domain is shown in Fig. 3(a), (b), which represents the Fig. 1 (left) and the rounding curved surface for symmetric volume, respectively. The grid near the annular orifice where the maximum velocity, and pressure gradients are, is refined as shown I, II, III in Fig. 3. Other cases with different control edges or structures were processed in the same way.

In the whole computational domain, the pressure inlet and pressure outlet are chosen as inlet and outlet boundary

conditions. The rest of the surfaces were defined as walls with no-slip condition. The fluid is the $46^{\#}$ anti-wear hydraulic oil with the density of 899 kg/m$^3$, and a kinematic viscosity of 46 mm$^2$/s. Two flow directions (from P to B and vice versa) are analyzed by inverting the inlet and outlet pressure boundary conditions. The convergence criteria was set to the residual values of continuity, $x$-velocity, $y$-velocity, $z$-velocity, and $k$ and epsilon were less than $10^{-5}$. Meanwhile, the mass flow rate difference between inlet and outlet was set less than $10^{-5}$ as one requisite convergence criteria to guarantee the conservation of mass.

RNG $k - \varepsilon$ model was used to predict the turbulence. In this study, the lowest Reynolds number is 346 at the annular orifice for all simulation conditions. This is higher than the critical Reynolds number, which ranges from 250 to 275 of the slide valve [26]. The RNG $k - \varepsilon$ model is the most suitable turbulence model for determining the valve flow features, as the flow inside a hydraulic valve is characterized by the coexistence of "free shear flows" due to the flow jet at the exit of the metering section [20]. The Enhanced Wall Treatment (EWT) is used as the near-wall treatment, as EWT provides consistent solutions for all $y+$ values, especially when using the $k - \varepsilon$ model for general single-phase fluid flow problems [27].

The governing equations were solved using the pressure-based solver. The SIMPLE scheme was selected for pressure-velocity coupling, and pressure discretization was produced by PRESTO!. The second-order upwind scheme was used to discretize the momentum, turbulent kinetic energy, and the turbulent dissipation equations.

Simulations were conducted for four different inlet pressures of 5, 10, 15, and 25 MPa, three types of control edges, two flow directions, and standard ports distribution (asymmetric) versus symmetric distribution. For slide valves with plated installation, the fluid flows from cylindrical inlet passage, as the internal flow and the inlet flow were fully developed, intensity and hydraulic diameter were chosen as the turbulence specification method. The hydraulic diameter was set to 20 mm equal to the diameter of the inlet port of the model, and the turbulent intensity was set to 8%. The value of turbulent intensity was estimated via the empirical correlation

$$I \equiv u'/u_{avg} = 0.16(Re_{D_H})^{-1/8} \tag{2}$$

where, $I$ is the turbulence intensity which is defined as the ratio of the root-mean-square of the velocity fluctuations $u'$, to the mean flow velocity $u_{avg}$, and $Re_{D_H}$ is the Reynolds number [27].

### B. GRID INDEPENDENCE ANALYSIS
Four different unstructured meshes with 0.37, 0.99, 2.5, and 5.7 million computational cells were created with the commercial software ANSYS Meshing, to investigate the mesh independence. These meshes are labeled with Grid 1 to Grid 4 in Fig. 4. The mesh independence simulations are conducted for a valve opening of 0.5 mm with outlet pressure being 0.1 MPa. The discretization error was estimated
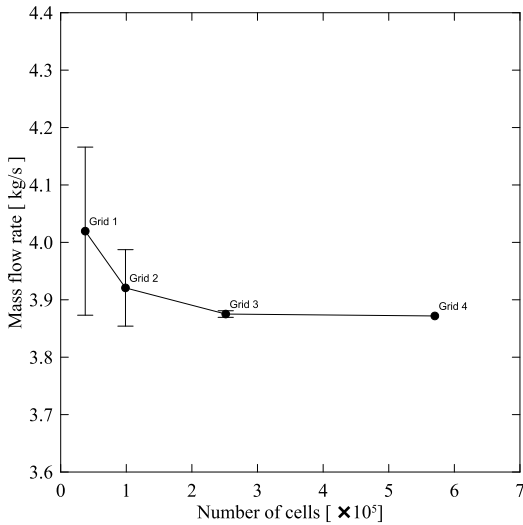
**FIGURE 4.** The mass flow rate comparison for grid independence analysis ($x$ = 0.5 mm, inlet pressure is set to 10 MPa and outlet pressure is set to 0.1 MPa).



**FIGURE 5.** Annular fluid domain cut from whole computational domain used as control volume for calculating radial flow force. (a) annular flow domain, (b) one-twelfth fluid domain of square land, (c)one-twelfth fluid domain of 45° conical surface, (d) one-twelfth fluid domain of rounding curved surface.

using the procedure presented by Celik *et al.* [28]. The mass flow rate was chosen as the studied variable. The error bars in Fig. 4 present the discretization error compared to the finest grid (Grid 4). The relative error of mass flow rate of Grid 3 is 0.08% compared to the Grid 4, and 1.2% and 2.5% for Grid 2 and Grid 1, respectively. Therefore, Grid 3 was selected for the rest of fluid domains with the same opening.

## IV. RESULTS AND ANALYSIS

### A. THE CONTROL VOLUME

The radial flow force here represents the flow force projecting perpendicular to the spool axis, which influences the lateral force. As flow velocity changes dramatically at the orifice, the pressure difference before and after orifice mainly determines the radial flow force according to Eq. (1). In order to calculate the force value, the annulus fluid domain selected as the control volume shown in Fig. 5, was cut from whole computational fluid domain, which is displayed in dashed-line rectangles in Fig. 1, and Fig. 2. The control volume chosen here has an advantage in that, the effects of the inner structure and oil passages location of the valve have been considered. This is more reliable than simulation results that held the assumption, that the fluid domain was completely symmetrical with the annulus being chosen as the only computational domain.

Fig. 5(a) shows the annulus fluid domain selected for force calculation in the outlet control mode. The red annular surface shown on the left side of the volume, is the pressure inlet; and the annular orifice opening, colored in green, is the pressure outlet. The inner and outer walls are part of the spool and housing surfaces, respectively. Fig. 5(b)–(d) represents one of twelfth areas of the control volumes for square land, 45° conical, and rounding curved control surfaces. It is obvious that the definition of the inlet and outlet boundaries should be exchanged in the inlet control condition. The pressure information was collected from the annulus fluid domain from the
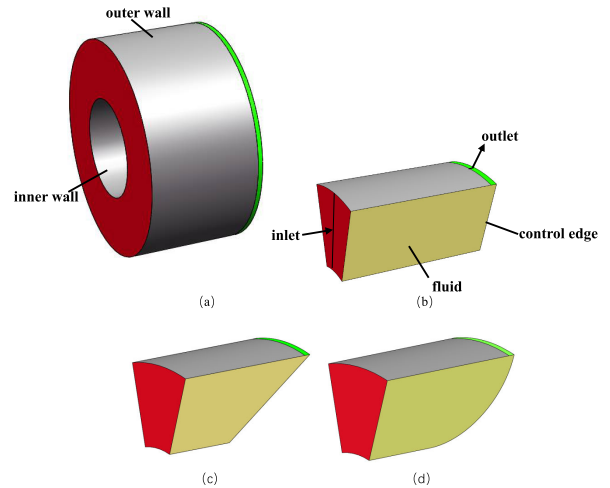
numerical results of both the inlet and outlet surfaces. In order to gather the flow force distribution around the orifice, six sections through the spool axis were created, whose locations were separated by an interval angle of 30 ° as shown on Fig. 6.
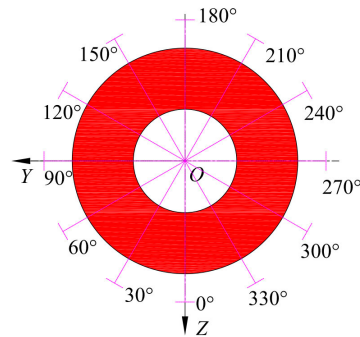


**FIGURE 6.** Six sections' positions of annular fluid domain through spool axis.

The pressure distributions on the twelve inlet and outlet lines are shown in Fig. 7, where the $X$-coordinate is the radial distance from the inner wall to the outer wall, and Fig. 8 where the $X$-coordinate is the distance of the orifice opening from the static housing control edge to the spool control edge under outlet control condition with rectangular edge, when the inlet pressure is 25 MPa and outlet pressure is 0.1 MPa. It is obvious that the pressure distributions at twelve inlet lines vary with the line position, while the pressure at twelve outlet lines at the annular orifice shows similar trends, but the values present differently.

The velocity at the orifice has a direct contribution to the fluid momentum, and is also used to determine the flow type as the definition of the Reynolds number. The twelve velocity distributions at the orifice along outlet lines under the same condition of Fig. 8 are shown in Fig. 9, this demonstrates that the flow is turbulent as the velocity values on the outlet line are close except at the two ends. Even though the velocity at the orifice was easy to acquire, the radial flow force in this
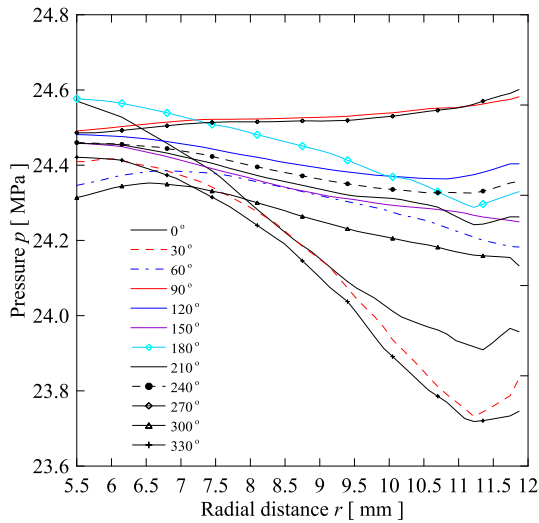
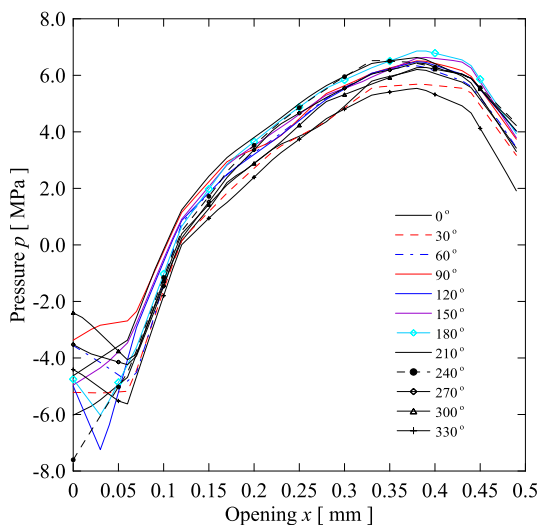**FIGURE 7.** Pressure distributions along the inlet edge.



**FIGURE 8.** Pressure distributions at the orifice along the spool axis from housing edge to spool control edge.



**FIGURE 9.** Velocity distributions at the orifice along the spool axis from housing edge to spool control edge.

port is directly connected to the tank. The mean radial flow force has a linear relationship as analyzed by authors in [23]. In the outlet control conditions, the radial flow force is smallest at the 45° conical control edge among three control profiles. On the contrary, the force on the spool with conical profile is highest among the three inlet control profiles.

Figure 11 shows the radial flow force variation along the periphery of the annular orifices under three control profiles of sliding spool, inlet, and outlet control cases when the inlet pressure was set to four different pressures. This indicates that the radial flow forces are much higher when fluid discharges out of the cavity, than when the fluid discharges out under the circumstances of the rectangular and round control edges. The radial flow force differences between inlet and outlet control modes under the 45 ° conical profile, are closer than the force differences of the other two profile types.

## C. NET RADIAL FLOW FORCE
As flow force has a direct connection with the velocity, and the direction of the force is determined by the direction of the velocity at the orifice, this results in the orifice opening closing [7], and thus the direction of radial flow forces on the spool is bound to point towards the spool axis and circumferential distribution. The force therefore, could self-compensate partially, but this will result in net radial flow force which should not be ignored as explained by Lu *et al.* [23]. The net radial flow force of each case was calculated by projecting the force at each position to the $Y$ and $Z$ directions, and summed up to achieve root-mean-square value according to formula 6. The values of net radial flow forces of all the simulation results are presented in Fig. 12.

work was calculated by using the pressure difference and not the velocity, as the velocity directions at inlet lines are not always parallel to the spool axis, and are hard to determine. In formula 1, the parameter jet angle was deduced by using overall velocity $v$, and the velocity u $v_x$ which projects in the $X$ direction as the Eq.3, $\Delta P$ is deduced by using the average pressure on the inlet edge minus the value on the outlet edge at the same position in Fig.5(b). Fig. 10 shows radial flow force variations along the orifice periphery under three types of control profiles, four different inlet pressures, metering-in and metering-out cases for the symmetric valve.

$$\theta = \mathrm{acos}\frac{v_x}{v} \qquad (3)$$

## B. RADIAL FLOW FORCE
Fig. 10(a) - (f) denotes the absolute radial flow force on the spool increases with inlet pressure, which also represents pressure difference; the outlet boundary here was set to an atmosphere that was suitable to the condition when the outlet
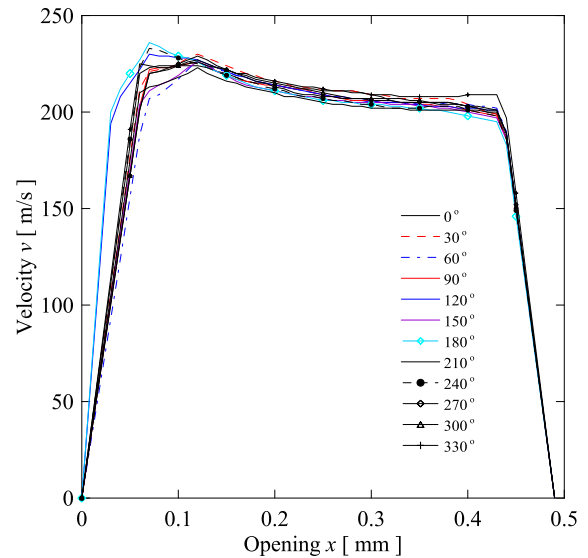
$$F_{rY} = -\sum F_r(\alpha)\mathrm{sin}\alpha \qquad (4)$$

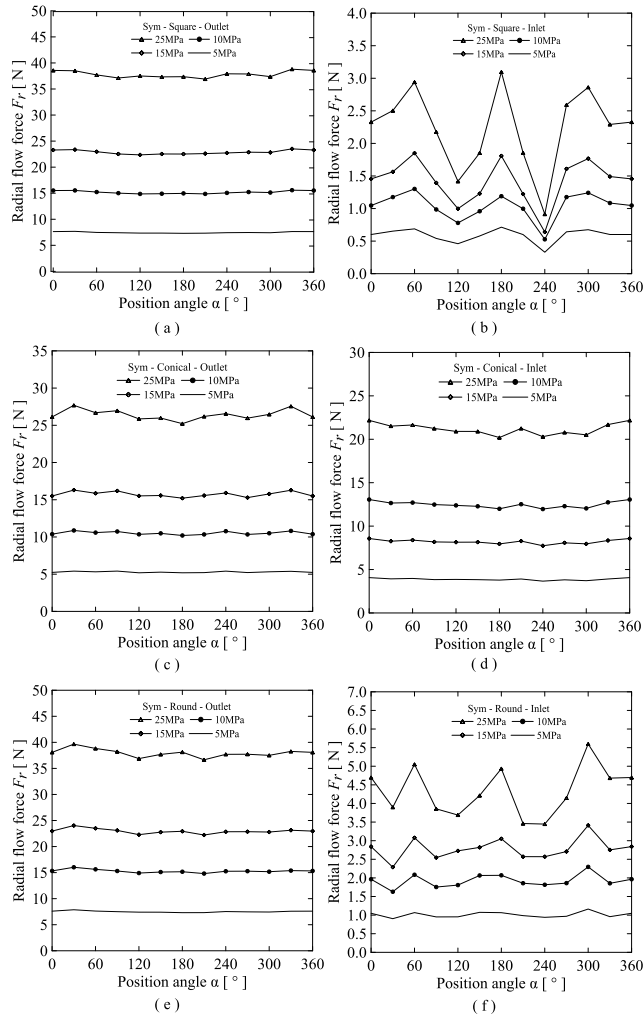$$F_{rZ} = -\sum F_r(\alpha)\mathrm{cos}\alpha \qquad (5)$$

**FIGURE 10.** Radial flow force distributions along orifice periphery of three profiles under different pressures and flow directions. ( a ) the square outlet control surface, ( b ) the square inlet control surface, ( c ) the 45° conical outlet control, ( d ) the 45° conical inlet control surface, ( e ) the rounding outlet control surface, ( f ) the rounding inlet control surface.

where $F_{rY}$ is the $Y$ component of the net radial flow force, and $F_{rZ}$ is the $Z$ component. Net radial flow force $F_{rn}$ acting on the spool at the orifice is the square root of the $F_{rY}$ and $F_{rZ}$ values, according to the formula (6):

$$F_{rn} = \sqrt{F_{rY}^2 + F_{rZ}^2} \qquad (6)$$

Fig. 12 demonstrates that the net radial flow force increases with the inlet pressure. The maximum net radial flow force is less than 4 N when the opening is 0.5 mm. And the force of asymmetric structures is less than 4 N under the same condition of symmetric structures, when the fluid flows out of the cavity. While the force in asymmetric structures is higher than that of symmetric structures, when the control edge profiles are rectangular and round, but the value of the conical profile shows the opposite.

## D. EFFECT OF THE PRESSURE DIFFERENCE
The pressure difference has a linear relationship with the radial flow force as shown in the formula 1. Fig. 13 shows the
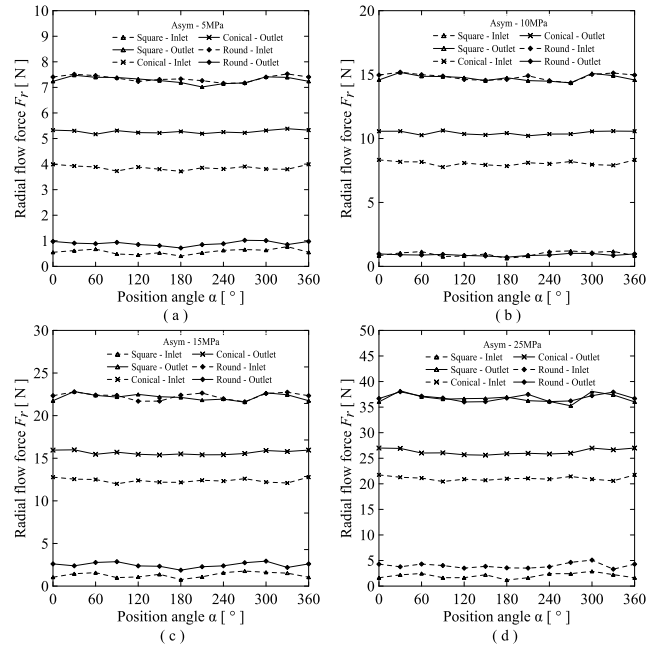


**FIGURE 11.** Radial flow force variations of three profiles, inlet and outlet control modes, and four pressures when the oil ports are asymmetric. (a) 5 MPa, (b) 10 MPa, (c) 15MPa, (d) 25 MPa.

average radial flow force from the values of twelve position changes with inlet pressure, when outlet pressure is set to atmospheric pressure. The straight lines of different simulation conditions present the linearity which goes well with the formula 1, and shows that the average radial flow force increases with the pressure difference. However, the slope of the lines in Fig. 13 varies with control surface profiles and flow directions, whereas straight lines are quite close under the same conditions except the symmetry of the cavity. The largest slope appears at the outlet control with rectangular and round control edges when the cavity is plane symmetry, while the slope is the least steep at the inlet control with the rectangular control edge. From formula 1, it expresses that the slope of the lines in Fig. 13 has a direct relation to $2C_q C_v \pi x \sin\theta$. However, the pressure difference extracted from the calculation of flow domain acts as a vital effect. One reason is that the jet angle $\theta$ is not always constant as shown in Fig.14, which is a critical factor on the slope in Fig.13.

In addition to the average radial flow force, the net radial flow force increases with the pressure difference demonstrating linearity in Fig. 12.

## E. EFFECT OF THE CONTROL SURFACE PROFILE
The radial flow forces show not only different values, but also different trends in the three profiles on the spool used for control surface. The force values of the square and round profiles under the outlet control case present a similar trend as shown in Figs. 10,11, and 12. The largest percentage error of average radial flow force between square and round profiles is 0.83 percent for the symmetric conical, and 0.82 percent for the asymmetric conical. However, for the inlet control case, the radial flow force at square control edge is lower than the
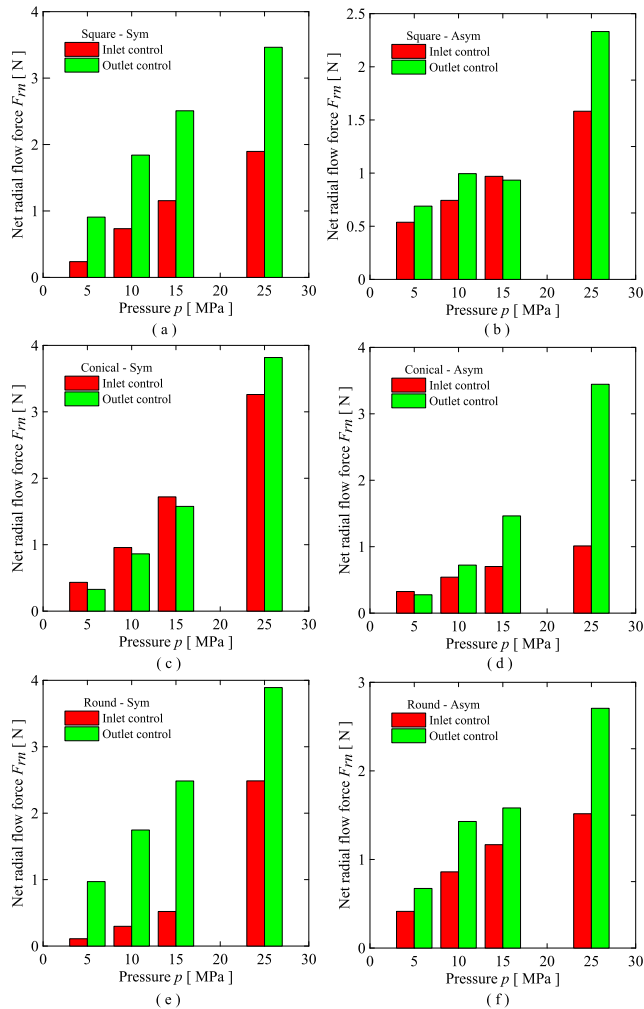
**FIGURE 12.** Net radial flow force of three types of control edges under different pressures and flow directions. (a)-(b) the rectangular control edge, (c)-(d) the conical control edge, (e)-(f) the round control edge.



**FIGURE 13.** The straight lines of average radial flow force with respect to pressure difference.

value at the round profile. The radial flow forces under the condition of conical control edge present differently with the other two profiles, which shows that the force value is higher than the other two inlet control cases, while smaller for outlet control edge.

For the square control profile, the radial flow force at the annular orifice of the inlet control mode, is much less than that of the value of outlet control for both symmetrical and asymmetrical valve structures. Fig. 13 shows the average radial flow force is 0.56 N for inlet control, and 7.45 N for outlet control for the symmetric structure when the inlet pressure is set to 5 MPa, and for the round control edge, the average flow force is 1.00 N and 7.51 N under the same condition. However, for the conical control edge, the average flow force for inlet control is 3.86 N, and 5.30 N for outlet control at 5 MPa inlet pressure with symmetric structure. Moreover, the value differences also increases with the pressure.

## F. EFFECT OF CAVITY SYMMETRY
The symmetric cavity of the sliding spool valve here has the feature that the inlet and outlet passages are machined on the
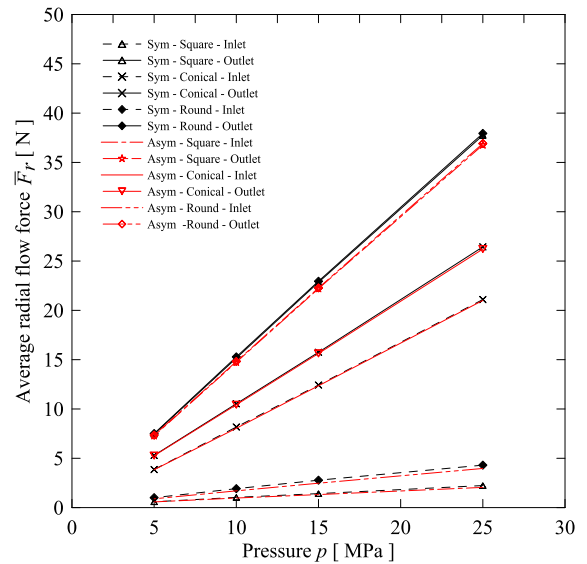
same section, and the other structure in which the passages are located on the respective sections according to ISO standard, is labeled with asymmetric valve. The average radial flow force which increases with pressure for the symmetric valve has similar tendencies to the asymmetric valve as shown in Fig. 13. The largest relative error for the square outlet control profile between the symmetric and asymmetric valves is 8.3 percent by using the average flow force when the inlet pressure is 25 MPa, the relative error decreases with the pressure. Thus the symmetry of the valve has little effect on the radial flow force. However, the net radial flow force which contributes to one actual lateral force caused by radial flow force is influenced by valve symmetry. The net radial flow force of the asymmetric valve is less than the value of the symmetric valve for each result shown in Fig. 12. The value of the square outlet control mode particularly, is at its minimum at 25 MPa, while the minimum value of the inlet control occurs at 25 MPa on the conical profile spool. There are two stagnation points on the symmetric plane for the symmetric valve [29], which in turn affects the pressure distribution around the spool, shown in Fig.20. This results in a larger pressure difference than the value of the asymmetric valve in which the stream flows around the spool surface in a helical manner without a typical stagnation point [17].

## G. EFFECT OF FLUID FLOW DIRECTION
The directional valve was designed with the ability to freely flow in two directions, the outlet control indicates when fluid discharges out, while the inlet control means that the fluid enters into the cavity. It is visible that the flow direction has a significant effect on the radial flow force as shown in Fig. 10, Fig. 11, and Fig. 13. The radial flow force of inlet control is much less than the value of the outlet control for the three types of control profiles, and the four different pressures. In Fig. 13, the average value of radial flow force

of outlet square control profile is 17.9 times the value of the inlet control case at 25 MPa, and 9.3 and 1.25 times the inlet control value, when the control surface is round and conical, respectively. The net radial flow force for the inlet control is less than the value for the outlet control edge in most cases, except for the conical control surface with symmetric volume, when pressure is less than 25 MPa.

The net radial flow force difference of the conical profile, which is the absolute value between inlet and outlet control cases at the same pressure, shows closest compared to the other two control profiles. The values are shown in Table 2 of three profiles when the pressure varies from 5 MPa to 25 MPa. It illustrates that the lesser the difference in the radial flow force, the closer the net radial flow force is.

**TABLE 2.** The net radial flow force differences.

| Pressure [ MPa ] | Net radial flow force difference | | |
|---|---|---|---|
| | Conical [ N ] | Square [ N ] | Round [ N ] |
| 5 | 0.11 | 0.67 | 0.86 |
| 10 | 0.09 | 1.11 | 1.45 |
| 15 | 0.14 | 1.35 | 1.96 |
| 25 | 0.56 | 1.57 | 1.40 |

## H. EFFECT OF JET ANGLE

The jet angle is a necessary part of determining the steady flow force, as it determines the direction of the flow velocity [26]. When the shoulder of the sliding spool was square land, the perimeter of the shoulder (75.4 mm) was larger compared to the opening of the orifice (0.5 mm). The flow was thus considered to be two-dimensional and the Laplace equation can be solved to determine the jet angle, which is presented in formula (7)

$$\frac{x}{c_r} = \frac{1 + \frac{\pi}{2}\sin(\theta) - \ln(\tan[\frac{\pi-\theta}{2}]\cos(\theta))}{1 + \frac{\pi}{2}\cos(\theta) + \ln(\tan[\frac{\pi/2-\theta}{2}]\sin(\theta))} \quad (7)$$

where the $c_r$, is the radial clearance between the valve and the valve housing (sleeve). From this equation, the jet angle varies between 21 to 69 degrees and for most valve openings, an angle of 69 degrees has been used as a good estimation for jet angle [26].

Jet angle is defined as the acute angle of the velocity vector at the orifice relative to the axial of the spool, and the angle is calculated according to equation (3). The average jet angle at the orifice for the round and square control surface is between 65 degrees and 68 degrees when the pressure difference increases from 5 MPa to 25 MPa. The angle values of the asymmetric and symmetric cavities are quite close for the square and round control profiles, shown in Fig. 14. However, the jet angle of the conical profile performs differently, the average value of which is around 56 degrees for inlet control, and 35 degrees for outlet control. In addition, the value decreases with the increasing of pressure for metering out which is opposite in the other cases.

It is indicated that the jet angle is not only influenced by the opening and the clearance for the spool valve, but also the pressure difference, and the control profile, which meant that formula 7 needed to be modified.
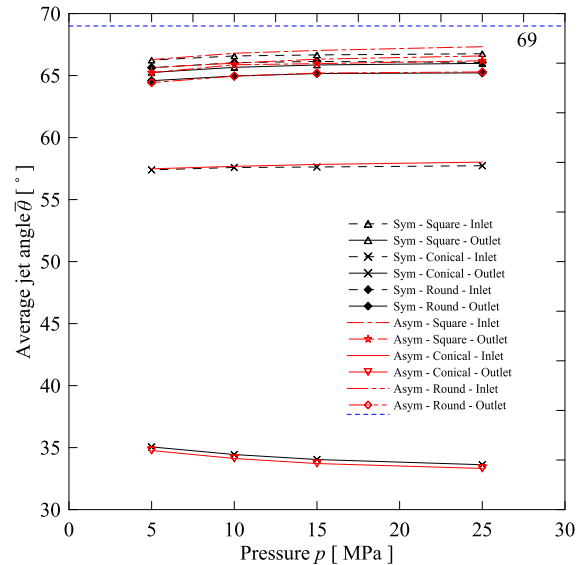


**FIGURE 14.** The relation between average jet angle and pressure difference.

## I. EFFECT OF STATIC PRESSURE ON THE SPOOL

The radial force on the spool surface plays a vital role in the valve design, as it increases the frictional resistance. The net radial force $\Sigma F_r$, which is also called the net lateral force, acting on the inner surface (spool surface), was directly calculated according to the simulation results presented in Fig. 12, by using root square value of forces in the $Y$ direction, and $Z$ direction, shown in Fig. 15. The net lateral force not only increases with increasing pressure, but is also a dozen times the net radial flow force at the annular orifice as shown in Fig. 13. It is obviously that the net lateral force varies from over 100 N to 300 N at 25 MPa. And the net lateral forces under conical profiles show less than the value under other two control surfaces' conditions in Fig. 15.

In order to figure out how the static pressure on the spool surface act on the lateral force. Pressure data are extracted from the two circles which are located on the spool surface at the inlet and outlet cross sections perpendicular to the axis showing in Fig. 17, the pressure variations along the circle are plotted in Fig. 16. Curves in Fig. 16 shows the static pressure on the spool is not uniformly circumferential, resulting in a lateral force on the spool.

The max static pressure differences shown in Fig. 16(a), (b) are calculated according to formula 8, by using the maximum static pressure $p_{smax}$ minus the minimum static pressure $p_{smin}$. The values are 0.095 MPa, 0.180 MPa, 0.225 MPa, and 0.045 MPa when the inlet pressures are 5 MPa, 10 MPa, 15 MPa, and 25 MPa, respectively. Meanwhile, Fig. 16(c), (d) show that the pressure differences at the outlet section on the valve surface are 0.231 MPa, 0.547 MPa, 0.896 MPa, and 1.437 MPa, respectively under four inlet pressures from 5 MPa to 25 MPa. The max static pressure difference shows linearity with inlet pressure as shown in Fig. 18. In addition, the ratio $r_{p_s}$ variation with static pressure difference $\Delta p_s$ versus inlet pressure $p_{in}$ as formula 9, is plotted in Fig. 18,
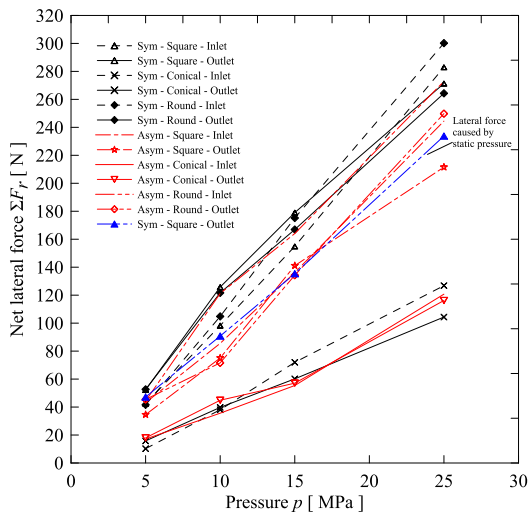
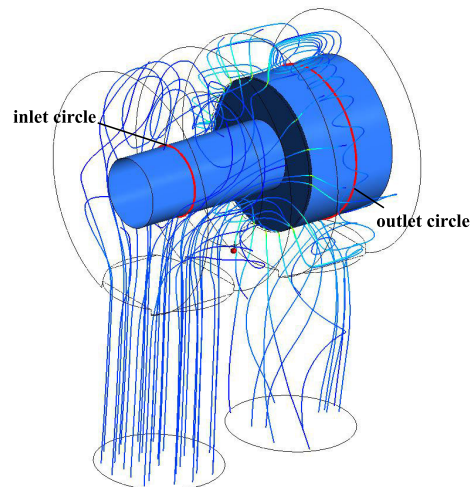**FIGURE 15.** The relation between lateral force and pressure difference.
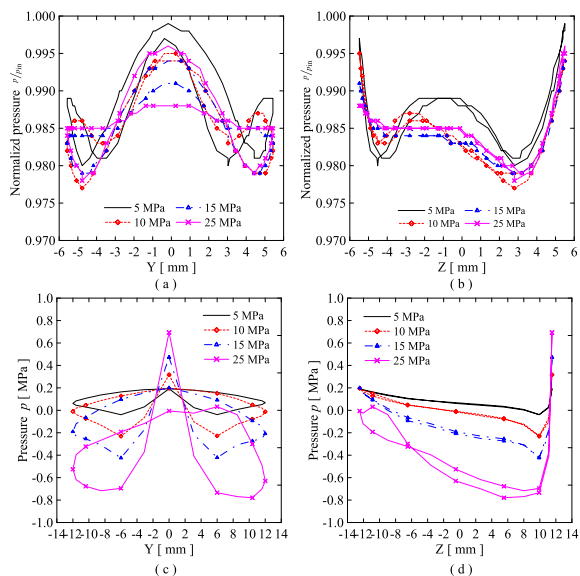


**FIGURE 16.** The static pressure variation on the spool surface at circle lines of the inlet and outlet sections when the control edge is rectangular at metering-out and symmetric condition. (a),(b) normalized pressure $p/p_{in}$ variation along $Y$ and $Z$ directions on the inlet line of the spool; (c),(d) pressure variation along $Y$ and $Z$ directions on the outlet line of the spool.

which confirms that the maximum static pressure difference on the spool has a linear relation with inlet pressure when outlet pressure is directly connected to the tank.

$$\Delta p_s = p_{smax} - p_{smin} \qquad (8)$$

$$r_{p_s} = \Delta p_s/p_{in} \qquad (9)$$

The pressure distribution on the inlet and outlet circle shown in Fig. 16 present symmetrically about plane $Y = 0$. If we assumed that the pressure distribution along the axis remains unchanged except at orifice area, the lateral force generated by static pressure could be estimated by using values in Fig. 16, and the surface area of the spool. The lateral force caused by static pressure was calculated, and shown in Fig. 15 under outlet control condition when the valve is symmetric. This verifies that the uneven static pressure
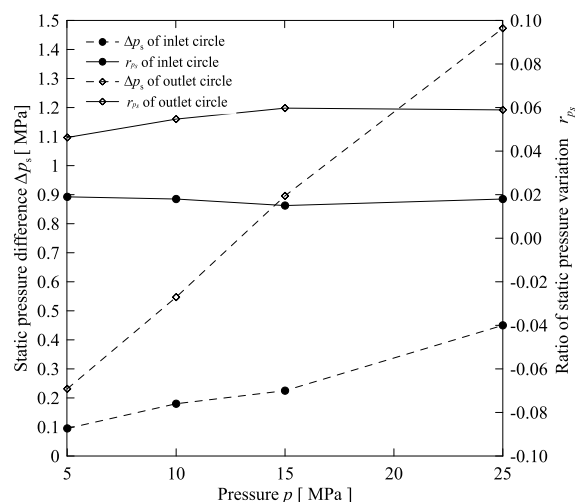


**FIGURE 17.** The position of inlet and outlet circles on the spool for acquiring static pressure.



**FIGURE 18.** The variation of static pressure difference and ratio of static pressure on inlet and outlet circles with inlet pressure.

distribution on the spool surface, plays a critical role in causing lateral force on the sliding spool.

## V. EXPERIMENTAL SETUP

To verify the computational simulation results of the static pressure distribution on the spool surface, the experimental test bed, whose hydraulic schematic diagram is shown in Fig. 19(a), was established with a prototype seat valve containing a special test channel made of nylon using a three-dimensional printer, as shown in Fig. 19(b). Because of the limited size of the prototype, seven valves were printed to cover seven circumferential test positions $\theta$ (180°, 210°, 240°, 270°, 300°, 330°, 360° (0°)), on the section through the outlet port axis, perpendicular to the spool axis.

All seven tested valves were printed with the same model size shown in Fig. 2, the orifice opening was 0.5 mm. The installation platform with a 3D-printed valve is shown in Fig. 19(c). In order to arrange the pressure sensor on the test rig, a transition valve block was fabricated, so as to connect the valve, and the pressure sensors. The features of
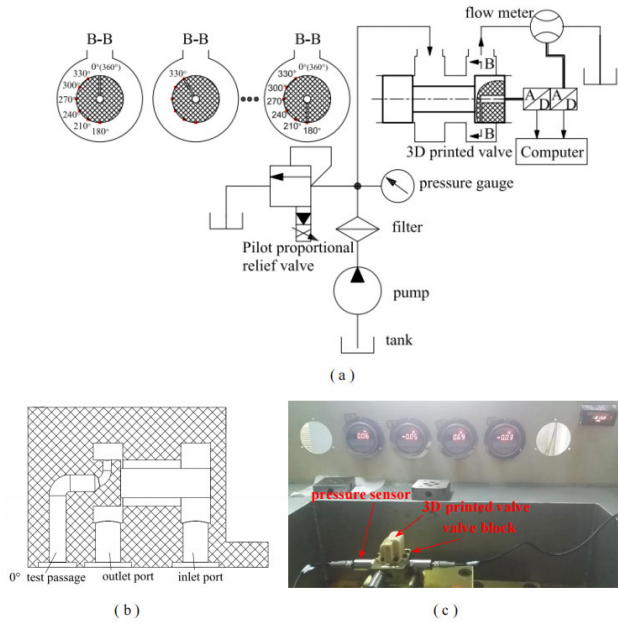
**FIGURE 19.** Hydraulic test bed. (a) the schematic diagram, (b) one section of 3D printed symmetric valve, (c) the platform for test.
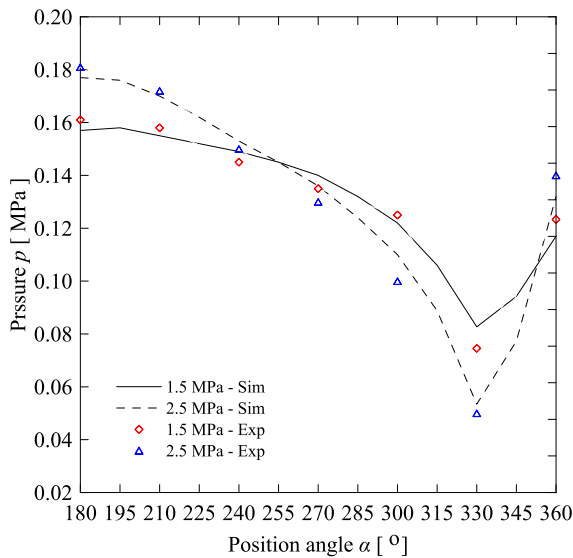


**FIGURE 20.** The experimental and simulation static pressure variations along half periphery of the outlet circle on the spool.

**TABLE 3.** Main sensors and equipment details.

| Description | Main features |
|---|---|
| Pressure gauge | HUBA511.940003142, 0-60bar, $< \pm 0.3\%$ FS |
| Flowmeter | VSE-1/16, 1-80 l/min, $< \pm 0.3\%$ measured value |
| DAQ module | USB-6363, 32 analog inputs, 16-bit, 2MS/s |

the pressure sensor and the flowmeter are listed in Table 3. The pressure sensors measured the pressure value at a specific position on the spool, as well as pressure of the inlet port. And the flowmeter measured the flow rate passing through the valve. All the signals were acquired using the NI USB 6363, a multi-function I/O device made by National Instruments, to the computer. Fig. 19(b) is the section of the prototype valve with test position 180°.

The leakage occurred on all outside surfaces of the 3D printed nylon valve during the experiment when the inlet pressure was over 3.0 MPa, except for the interface between tested valve and block. Due to this, the pressure test was carried out with an inlet pressure below 3 MPa. Fig. 20 presents experimental and tested results of the static pressure variations with the angle position on the spool surface at the outlet circle when the inlet pressure was 1.5 MPa and 2.5 MPa. It showed that the pressure reached a maximal value at the angle position of 180°, and decreased along the cylindrical surface reaching a minimum value around 330°, finally, the pressure reached a peak value at 360° (0°), the two maximal values are two stagnation points as explained in [29]. It is visible that the static pressure changes around the cylindrical surface of the spool, and the amplitude of the variation increased with inlet pressure, which was verified by the experiment and provides the explanation; the variable static pressure on the spool contributions radial force unbalance for the sliding-spool, should be considered when selecting the electoral-mechanical actuator.

## VI. CONCLUSION

In this study, the effect of the lateral force on the sliding-spool valve was analyzed. The results indicated that

1) the radial flow force varies linearly with pressure difference.
2) the jet angle was not only influenced by the clearance and opening, but was also affected by the control surface profile, and flow direction.
3) the radial flow force on the spool under the inlet control mode was less than the value under outlet control, and the force difference between inlet and outlet control of conical profile was the least compared to the other two profiles.
4) the static pressure is an important contributing factor in the lateral flow force to the spool, and the amplitude of static pressure variation increases linearly with pressure difference.

The results demonstrated that the lateral force on the spool is affected by radial flow force, and static pressure distribution on the cylindrical surface. When the opening is 0.5 mm, the maximum net radial flow force is less than 4 N which is much smaller, compared to the lateral force caused by static pressure with the value of 228 N when the inlet pressure is 25 MPa. These results completed the factors which caused the lateral force, by adding radial flow force, and static pressure on the sliding spool, in order to precisely evaluate the resistances that should be overcome by the actuator.

Further research should focus on the theoretical analysis of radial flow force, and static flow force acting on the spool, which would help to fulfill the mathematical models of sliding valves, helping to select a more appropriate actuator.

## REFERENCES
[1] H. Gao, B. Li, and G. Yang, "Study on the influence of flow force on a large flowrate directional control valve," *IFAC Proc. Volumes*, vol. 46, no. 5, pp. 469–477, 2013.

[2] N. D. Manring and R. C. Fales, *Hydraulic Control Systems*. Hoboken, NJ, USA: Wiley, 2019.

[3] H. E. Merritt, *Hydraulic Control Systems*. New York, NY, USA: Wiley, 1967.

[4] N. Heraković, "Flow-force analysis in a hydraulic sliding-spool valve," *Strojarstvo*, vol. 51, no. 6, pp. 555–564, 2009.

[5] J. Lugowski, "Steady-state flow-force compensation in a hydraulic spool valve," 2013, *arXiv:1312.1310*. [Online]. Available: https://arxiv.org/abs/1312.1310

[6] J. Lugowski, "Flow-force compensation in a hydraulic valve," in *Proc. ASME BATH Symposium*, 2015, pp. 1–7.

[7] J. Lugowski, "Flow force in a hydraulic spool valve," in *Proc. ASME-JSME-KSME Joint Fluids Eng. Conf.*, 2019, pp. 1–9.

[8] H. Xie, L. Tan, J. Liu, H. Chen, and H. Yang, "Numerical and experimental investigation on opening direction steady axial flow force compensation of converged flow cartridge proportional valve," *Flow Meas. Instrum.*, vol. 62, pp. 123–134, Aug. 2018.

[9] L. Tan, H. Xie, H. Chen, and H. Yang, "Structure optimization of conical spool and flow force compensation in a diverged flow cartridge proportional valve," *Flow Meas. Instrum.*, vol. 66, pp. 170–181, Apr. 2019.

[10] Q. Yuan and P. Y. Li, "Using steady flow force for unstable valve design: Modeling and experiments," *J. Dyn. Syst., Meas., Control*, vol. 127, no. 3, pp. 451–462, Sep. 2005.

[11] E. Frosina, A. Senatore, D. Buono, M. Pavanetto, and M. Olivetti, "3D CFD transient analysis of the forces acting on the spool of a directional valve," *Energy Proc.*, vol. 81, pp. 1090–1101, Dec. 2015.

[12] E. Frosina, G. Marinaro, A. Senatore, and M. Pavanetto, "Numerical and experimental investigation for the design of a directional spool valve," *Energy Proc.*, vol. 148, pp. 274–280, Aug. 2018.

[13] Y. Zhang, S. Wang, J. Shi, and X. Wang, "Evaluation of thermal effects on temperature-sensitive operating force of flow servo valve for fuel metering unit," *Chin. J. Aeronaut.*, vol. 33, no. 6, pp. 1812–1823, Jun. 2020.

[14] S. Fan, R. Xu, H. Ji, S. Yang, and Q. Yuan, "Experimental investigation on contaminated friction of hydraulic spool valve," *Appl. Sci.*, vol. 9, no. 23, p. 5230, Dec. 2019.

[15] L. Lu, F. Xia, Y. Yin, J. Yuan, and S. Guo, "Spool stuck mechanism of ball-type rotary direct drive pressure servo valve," (in Chinese), *J. ZheJiang Univ., Eng. Sci.*, vol. 53, no. 7, pp. 1265–1273, 2019.

[16] T. Siwulski, "Study on the friction forces in a spool-sleeve pair of hydraulic directional control valve," in *Proc. 24th Int. Conf. Eng. Mech.*, vol. 144, 2018, pp. 761–764.

[17] J. Rajda and E. Lisowski, "Flow forces acting on the spool of directional control valve," *Czasopismo Techniczne*, vol. 5, pp. 349–356, 2013.

[18] *Hydraulic Fluid Power—Four- and Five-Port Servovalves—Mounting Surfaces*, Standard ISO 10372:1992, International Organization for Standardization, Geneva, Switzerland, 2017.

[19] R. Amirante, G. Dal Vescovo, and A. Lippolis, "Flow forces analysis of an open center hydraulic directional control valve sliding spool," *Energy Convers. Manage.*, vol. 47, no. 1, pp. 114–131, Jan. 2006.

[20] R. Amirante, G. Del Vescovo, and A. Lippolis, "Evaluation of the flow forces on an open centre directional control valve by means of a computational fluid dynamic analysis," *Energy Convers. Manage.*, vol. 47, nos. 13–14, pp. 1748–1760, Aug. 2006.

[21] R. Amirante, L. A. Catalano, and P. Tamburrano, "The importance of a full 3D fluid dynamic analysis to evaluate the flow forces in a hydraulic directional proportional valve," *Eng. Comput.*, vol. 31, no. 5, pp. 898–922, Jul. 2014.

[22] R. Amirante, E. Distaso, and P. Tamburrano, "Sliding spool design for reducing the actuation forces in direct operated proportional directional valves: Experimental validation," *Energy Convers. Manage.*, vol. 119, pp. 399–410, Jul. 2016.

[23] Q. Lu, J. Tiainen, M. Kiani-Oshtorjani, and J. Ruan, "Radial flow force at the annular orifice of a two-dimensional hydraulic servo valve," *IEEE Access*, vol. 8, pp. 207938–207946, 2020.

[24] R. Fitzpatrick, *Theoretical Fluid Mechanics*. Bristol, U.K.: IOP Publishing, 2017, pp. 2053–2563.

[25] S. Y. Lee and J. Blackburn, "Contributions to hydraulic control 1 steady-state axial forces on control-valve pistons," *Trans. ASME*, vol. 8, pp. 1005–1011, Aug. 1952.

[26] H. Sigloch, *Technische Fluidmechanik*, vol. 6. Berlin, Germany: Springer, 2009.

[27] *ANSYS Fluent User's Guide, Release 19.2*, ANSYS, Inc., Canonsburg, PA, USA, 2018.

[28] I. B. Celik, U. Ghia, P. J. Roache, and C. J. Freitas, "Procedure for estimation and reporting of uncertainty due to discretization in CFD applications," *J. Fluids Eng.-Trans. ASME*, vol. 130, no. 7, pp. 078001-1–078001-4, 2008.

[29] Q. Lu, J. Ruan, and S. Li, "Research on radial forces for hydraulic slide valves caused by Bernoulli effect," *Chin. Mech. Eng.*, vol. 28, no. 19, pp. 2332–2338, 2017.
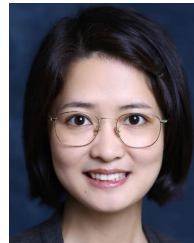
**QIANQIAN LU** was born in Anhui, China, in 1985. She received the bachelor's degree in mechanical design and automation from Northeastern University, Shenyang, China, in 2007, the M.Sc. degree in mechatronics engineering from Zhejiang University, Hangzhou, China, in 2010, and the Ph.D. degree from the School of Mechanical Engineering, Zhejiang University of Technology, Hangzhou, in 2019.

In 2010, she has worked as a Lecturer at Zhejiang University City College, Hangzhou, and promoted as an Associate Professor, in 2021. She worked as a Visiting Scholar at Lahti University of Technology (LUT), Lappeenranta, Finland, in 2020. Her current research interests include fluid mechanics, computational fluid dynamics, hydraulic components, and hydraulic transmission and control.

**JONNA TIAINEN** received the D.Sc. degree in heat transfer and fluid dynamics from Lahti University of Technology (LUT), Lappeenranta, Finland, in 2018.

She is currently working as a Postdoctoral Researcher with the Laboratory of Fluid Dynamics, LUT. Her research concentrates on turbomachinery. Her research interests include energy storage technologies and waste heat recovery.

**MEHRAN KIANI-OSHTORJANI** was born in Isfahan, Iran, in 1991. He received the B.Sc. degree from Yazd University, in 2013, the M.Sc. degree from Sharif University of Technology, in 2015, and the D.Sc. degree from Lahti University of Technology (LUT), Lappeenranta, in 2020.

He has been a Postdoctoral Researcher at LUT, since 2021. Since then, he has also been working at Oilon Group Oy as a Research and Development Engineer. He is an Expert in algorithm design and professional in scientific programming. He is interested in CFD, machine-learning algorithms, fluid power systems, energy systems, dynamic and thermal behaviour of granular materials, multi-phase flows, and their real-time simulations.

**YANGFANG WU** was born in Zhejiang, China, in 1974. She received the bachelor's degree in mechanical design and automation from Harbin Engineering University, Harbin, China, in 1996, and the M.Sc. degree in mechanical manufacturing and automation from Zhejiang University, Hangzhou, China, in 2003, where she is currently pursuing the Ph.D. degree in engineering.

Since 2011, she has been working as an Associate Professor with Zhejiang University City College, Hangzhou. Her current research interests include sensors and actuators, mechanics, and signal processing.

● ● ●